The 3D Channel Framework Based on Indium(III)–btec, and Its Ion-Exchange Properties (btec = 1,2,4,5-Benzenetetracarboxylate)

Zheng-zhong Lin,[a] Fei-long Jiang,[a] Da-qiang Yuan,[a] Lian Chen,[a] You-fu Zhou,[a] and Mao-chun Hong*[a]

Keywords: Indium / Benzenetetracarboxylate / Crystal structure / Ion exchange / Pyridine derivatives

Hydrothermal reactions of $InCl_3$ with pyromellitic dianhydride and pyridine derivatives produce three coordination polymers: $\{(HL)[In_3(btec)_2(OH)_2]\cdot L\}_n$ [btec = 1,2,4,5-benzenetetracarboxylate, L = 2-picoline (**1**), L = 4-picoline (**2**)] and $\{(Hdpea)[In_3(btec)_2(OH)_2]\}_n$ [dpea = 1,2-bis(4-pyridyl) ethane] (**3**). Single crystal X-ray diffraction and powder X-ray diffraction analyses reveal that compounds **1**–**3** are isostructural and possess the same 3D framework as 1D open channels. Thermal gravimetric studies show that compounds **1**–**3** are stable up to 300 °C. The guests of the protonated pyridine derivatives located at the channels in **1** and **2** can be fully exchanged by Ca^{2+} and Ba^{2+} ions.

Introduction

The construction of porous structures or open frameworks with new sizes, shapes, and chemical environments that can undergo solvent removal, solvent inclusion, solvent absorption, or ion exchange[1–4] represents one of the most challenging subjects in recent years. In this regard, various carboxylate-containing ligands, including 1,2,4,5-benzenetetracarboxylic acid (H_4btec), have been used in the assembly of such robust frameworks. H_4btec, which exhibits variation in the possible binding mode of the four acid groups and a strong tendency to form large, tightly bound metal cluster aggregates, has been applied as an organic component to construct porous coordination frameworks.[5] Moreover, the rigid conformation of H_4btec endows robustness to the resulting frameworks to make them thermally stable. With the aim of thoroughly investigating the coordination chemistry of H_4btec, we recently began studies on the assembly reactions of H_4btec with indium metal ions. The reason we selected indium(III) is that, in spite of the enormous number of coordination polymers assembled from divalent metal and H_4btec,[6–8] the field of indium(III) with btec ligands remains unexplored. Furthermore, it was postulated that the incorporation of trivalent metal ions might create diverse structures strikingly different from those containing divalent metal ions because of the increased valence charge of the metal centers. The indium ion is liable to hydrolyze, which limits its use in the construction of coordination polymers. However, by adding an appropriate basic reagent to deprotonate H_4btec and carefully controlling the reaction conditions, we have found that indium(III) ions can be used to construct the new frameworks. Herein we report three novel coordination polymers: $\{(HL)[In_3(btec)_2(OH)_2]\cdot L\}_n$ (**1**, L = 2-picoline; **2**, L = 4-picoline), and $\{(Hdpea)[In_3(btec)_2(OH)_2]\}_n$ [**3**, dpea = 1,2-bis(4-pyridyl)ethane]. Complexes **1**–**3** bear the same 3D channel frameworks. The protonated organic guests in complexes **1** and **2** can be fully exchanged by certain inorganic ions. Although a number of compounds based on {M–btc}[3c] or {M–1,4-bdc}[9] (M = metal ions, btc = 1,3,5-benzenetricarboxylate, and 1,4-bdc = 1,4-benzenedicarboxylate) systems are capable of guest exchange, the exchange behavior reported here is rarely found in the coordination polymers based on {M–btec}.

[a] State Key Laboratory of Structural Chemistry, Fujian Institute of Research on the Structure of Matter, Chinese Academy of Sciences, Graduate School of the Chinese Academy of Sciences, Fujian, Fuzhou 350002, China
Fax: +86-591-8371-4946
E-mail: hmc@fjirsm.ac.cn

Results and Discussion

Syntheses and Crystal Structures

The hydrolysis reaction of pyromellitic dianhydride under hydrothermal conditions gives H_4btec, which further aggregates with indium(III) ions to produce compounds **1**–**3**. The in situ method of using pyromellitic dianhydride to synthesize {M–btec} compounds has been reported before.[10] The preparation depends on the pH value of the starting reaction mixture. Pyridine derivatives are added to adjust the pH value and act as templates. So the amount of pyridine derivatives is vital, and the proper pH value ranges between 5 and 6. With a pH value lower than 3 the reaction systems of compounds **1**–**3** produce a byproduct with a 3D structure formulated as $[In_2(H_2btec)_2(OH)_2]_n\cdot 2n\,H_2O$.[11] Thus, to ensure the purity of compounds **1**–**3**, an excessive amount of pyridine derivatives is needed.

As compounds **1**–**3** possess the same framework, compound **2** is selected to represent their structures. There are two kinds of indium coordination environments: the In1 center is bonded to four oxygen atoms from four $btec^{3-}$ ligands, and to two μ_3-OH groups (O9 and its symmetrically equivalent atom) to form a distorted octahedral geometry. Two μ_3-OH groups occupy the axial positions of an octahedron. The In2 center is coordinated to five oxygen atoms from four $btec^{3-}$ ligands, and two μ_3-OH groups to form a pentagonal bipyramidal motif. The two axial positions are occupied by a μ_3-OH group and a carboxylate oxygen atom (Figure 1). The In–O distances range from 2.094(5) to 2.314(5) Å, compatible with those observed in other In^{III}–carboxylate complexes.[12] Bond valence sum (BVS) calculations[13] confirm that all indium ions have an oxidation state of +3. To balance the charge, O9 can be considered to be a μ_3-OH group. This assumption is confirmed by BVS for O9, which gives a result of 1.22. The four carboxylate arms of the btec ligand are all deprotonated, two of them bidentately bind to four indium ions, and the other two adopt the chelating bidentate mode and the monodentate mode (Figure 1). The two μ_3-OH groups bridge indium ions to form an In_4O_{22} tetranuclear cluster in which four indium ions (two In1 and two In2) are in a plane. The two μ_3-OH groups are located at both sides of the plane (Figure 2). If four tetranuclear clusters and eight btec ligands are conceptually viewed as edges, then a subunit similar to a right prism is obtained (Figure 3). Four In1 vertexes are connected by four btec groups to give the rhombic top side of the prism. All btec benzene rings are perpendicular to the top side. The centroids of the four benzene rings connected to the In1 vertexes lie above and below the top side. Above the top side are two neighboring btec benzene rings whose centroids are situated at $x = 0.12608$; the other two btec benzene rings below the top side are located at $x = -0.12608$ (Figure 4). These two positions are related through the centrosymmetric operation. This situation can also be found

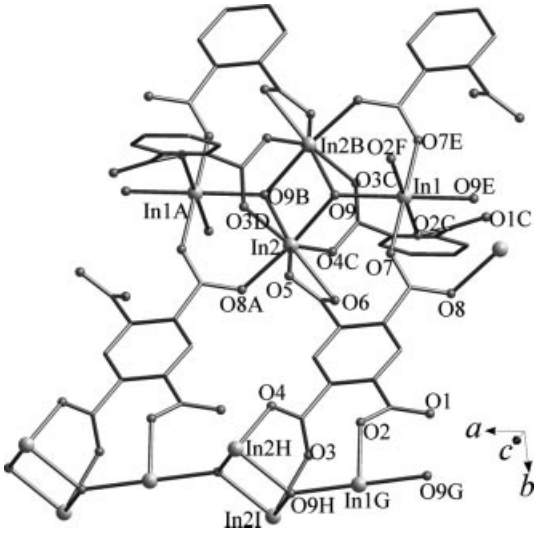

Figure 1. Coordination environment of indium ions in compound **2**. Symmetry code: (A) 1+*x*, *y*, *z*; (B) 1 – *x*, 1 – *y*, –*z*; (C) *x*, 1.5 – *y*, –0.5 + *z*; (D) 1 – *x*, –0.5 + *y*, 0.5 – *z*; (E) –*x*, 1 – *y*, –*z*; (F) –*x*, –0.5 + *y*, 0.5 – *z*; (G) –*x*, 0.5 + *y*, 0.5 – *z*; (H) *x*, 1.5 – *y*, 0.5 + *z*; (I) 1 – *x*, 0.5 + *y*, 0.5 – *z*. For clarity only two carboxylate arms of a part of the btec groups are drawn.

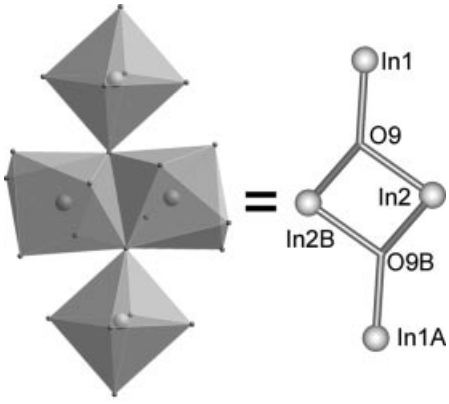

Figure 2. In_4O_{22} tetranuclear cluster and its conceptual representation. In1···In1A= 7.203 Å, In2···In2B = 3.268 Å

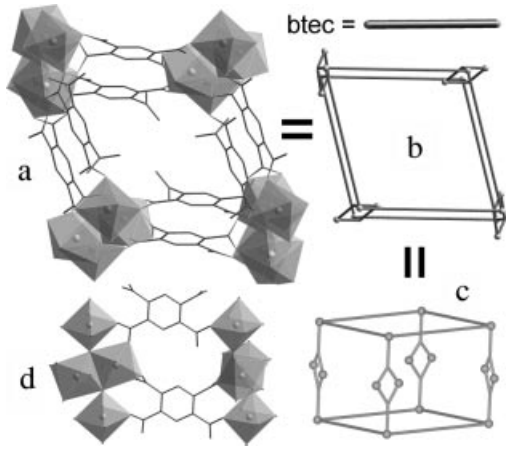

Figure 3. (a) A subunit constructed from four In_4O_{22} tetranuclear clusters and eight btec groups. In the subunit the opposite benzene rings are parallel to each other. It can be seen that the plane defined by four In ions in a tetranuclear clusters is parallel to the plane in the opposite tetranuclear cluster and perpendicular to the plane in the neighboring tetranuclear cluster. (b) The conceptual representation of a right prism for the subunit. (c) Front view of the right prism. (d) The detailed show of one lateral side of the prism.

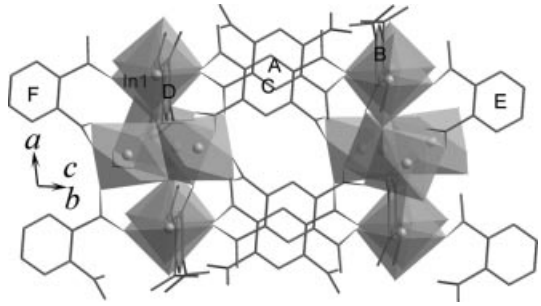

Figure 4. Demonstration of the positions of the btec groups surrounding a prism. Benzene rings A and B are located above the top side and benzene C–F below the top side. For clarity only two carboxylate arms of the lateral btec groups are drawn.

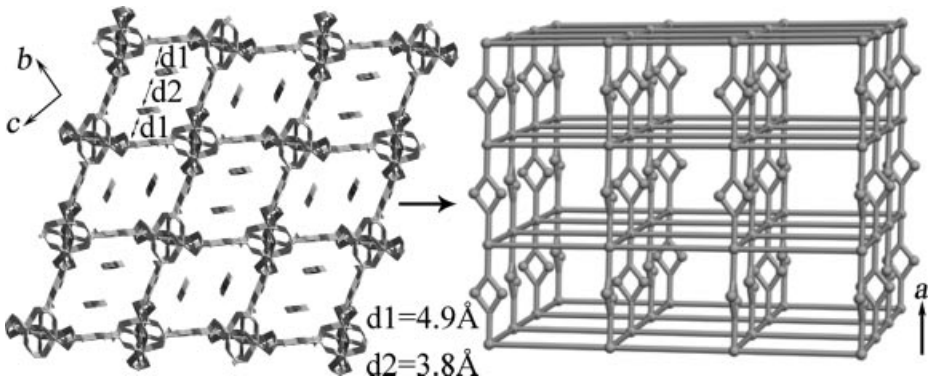

Figure 5. (left) View of a 3-D network in **2** with 1-D channels containing H4pic guests and (right) its conceptual representation (H4pic guests are omitted for clarity; note that the view directions of these two drawings are different).

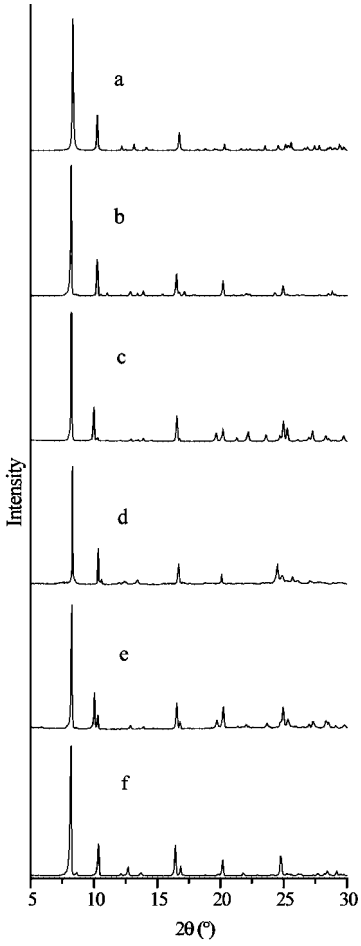

Figure 6. XRPD patterns of compounds **1**–**3**: (a) calculated pattern based on $[In_3(btec)_2(OH)_2]^-$ framework, (b) experimental pattern of **1**, and (c) pattern of the exchanged product of **1** with Ba^{2+}, (d) experimental pattern of **2**, and (e) pattern of the exchanged product of **2** with Ba^{2+}, (f) experimental pattern of **3**.

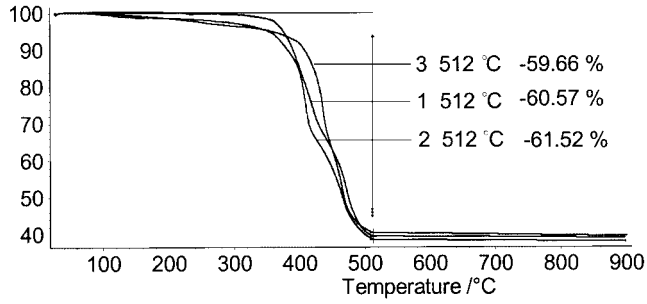

Figure 7. TG curves of **1–3** measured under flowing air.

when arranging the four btec benzene rings connected to the bottom-side In1 vertexes. Prisms are extended along [100], [011], and [0$\bar{1}$1] directions to generate a 3D network (Figure 5) containing the planar layers defined by In1 ions. By sharing In1 vertexes, tetranuclear clusters are extended through the crystallographic *a* axis to give infinite chains which act as pillars to support the planar layer. The shortest contact between the pillars is 5.496 Å (O4···O5). The btec groups reproduced along the [011] axis are alternately arranged above and below the In1 planar layer. This also applies to the btec groups reproduced along the [0$\bar{1}$1] direction. In such an arrangement mode, the btec groups fill in the space between the pillars and therefore prevent the framework from generating channels along the [011] and the [0$\bar{1}$1] directions. The only channel runs through the crystallographic *a* axis with diagonal dimensions as long as 13.425×17.544 Å^2. The organic guests, protonated pyridine derivatives, reside in the channels. The pyridine rings are parallel to each other and the centroid-to-centroid distances are longer than 4.5 Å, indicating no π–π contacts between pyridine rings. However, the centroid-to-centroid distances between pyridine rings and the nearest opposite btec benzene rings are 3.790 Å, indicating strong π–π contact. The nitrogen atoms in pyridine rings have no hydrogen bond interactions with the oxygen atoms in the framework. On the basis of PLATON calculations,[14] the solvent accessible volume constitutes 43.3% of the total crystal volume.

The homogeneities of compounds **1**–**3** are confirmed by X-ray powder diffraction (XRPD) patterns (Figure 6). The fact that the powder patterns obtained experimentally are in good agreement with the calculated patterns indicates that these three compounds are isostructural coordination polymers with the same 3D frameworks.

Thermal gravimetric (TG) data for compounds **1**–**3** under flowing air are shown in Figure 7. From 360 to 512 °C, compounds **1**–**3** dramatically lose the weight of both organic guests and btec ligands simultaneously. Powder X-ray diffraction for their residues shows that **1**–**3** are finally transformed to In_2O_3 after being heated at 512 °C. The total weight loss of **1**, **2**, and **3** is about 39.43%, 38.48%, and 40.34%, respectively, consistent with the calculated value of In_2O_3 (about 39.1%).

Ion-Exchange Analysis

In a typical ion-exchange experiment, original samples (about 25 mg) of compounds **1**–**3** were each immersed in a solution of $CaCl_2$ and $BaCl_2$ (10 mL, 1.0 M) for one day at 60 °C. The products were filtered, washed with distilled water and then dried in air. After exchange experiments, compounds **1** and **2** became less crystalline, while **3** remained in its crystalline form. Elemental analysis indicates that the guest cations in **1** and **2** can be fully exchanged by Ca^{2+} and Ba^{2+} ions, reflected by the significant decrease in C and N content. Only slight changes in C and N content[15] were observed for the exchanged sample of **3**, indicating that **3** cannot undergo ion exchange. The Hdepa molecule has a larger size than H2pic and H4pic; this inhibits it from moving freely along channels and therefore reduces its exchange ability. The major XRD reflections (Figure 6) of **1** and **2** can also be observed in their sample exchanged with Ba^{2+}, indicating that in both **1** and **2** the $[In_3(btec)_2(OH)_2]^-$ framework remains unchanged after the exchange.

Experimental Section

Preparation: A mixture of $InCl_3{\cdot}4H_2O$ (74.0 mg, 0.25 mmol), pyromellitic dianhydride (55 mg, 0.25 mmol), 2-picoline (typical example: 0.8 mL, 8 mmol), and H_2O (5.0 mL) in a 30-mL Teflon-lined stainless steel vessel was heated at 165 °C for 85 h, and then was cooled to room temperature at a rate of 6 °C·h^{-1}, giving light yellow prism crystals of **1**. The crystals were collected by density difference and washed with *N*,*N*-dimethylformamide (DMF) and water sequentially, giving an isolated yield of 62 mg (70%) based on $InCl_3{\cdot}4H_2O$. Compounds **2** and **3** were prepared in a similar way simply by replacing 2-picoline with 4-picoline (0.8 mL, 8 mmol) or with a mixture of pyridine (0.1 mL, 1.2 mmol) and dpea (368 mg, 2 mmol) and obtained in the yields of 60 mg (68%) and 53 mg (60%), respectively, based on $InCl_3{\cdot}4H_2O$. **1**: $C_{32}H_{21}In_3N_2O_{18}$ (1065.97): calcd. C 36.03, H 1.99, N 2.63; found C 36.22, H 2.12, N 2.66. IR (KBr): $\tilde{\nu}$ = 3503 (br), 3054 (m), 1613 (s), 1589 (vs), 1499 (s), 1411 (s), 1371 (vs), 1317 (m), 1252 (m), 1141 (m), 878 (w), 805 (m), 761 (m) cm^{-1}. **2**: $C_{32}H_{21}In_3N_2O_{18}$ (1065.97): calcd. C 36.03, H 1.99, N 2.63; found C 35.81, H 2.10, N 2.58. IR (KBr): $\tilde{\nu}$ = 3606 (m), 3523 (m), 3221 (m), 3086 (m), 1636 (m), 1595 (vs), 1548 (s), 1505 (m), 1427 (s), 1382 (s), 1337 (s), 1135 (m), 1005 (m), 941 (m), 857 (m), 805 (m), 779 (m), 755 (m) cm^{-1}. **3**: $C_{32}H_{19}In_3N_2O_{18}$ (1063.97): calcd. C 36.12, H 1.80, N 2.63; found C 36.44, H 2.10, N 2.67. IR (KBr): $\tilde{\nu}$ = 3422 (m), 3327 (m), 3129 (m), 1615 (s), 1590 (s), 1552 (sh, vs), 1497 (s), 1402 (s), 1373 (s), 1317 (m), 1140 (m), 932 (m), 878 (m), 815 (m), 761 (m) cm^{-1}.

Crystallographic Studies: Intensity data of **2** and **3**[16] were collected with a Rigaku mercury CCD diffractometer with graphite-monochromated Mo-K_α (λ = 0.71073 Å) radiation by using the ω–2θ scan method at room temperature. The structures were solved by direct methods using SHELXS-97[17a] and were refined on F^2 by the full-matrix least-squares methods SHELXL-97.[17b] Because of a disorder problem, some atoms of the dpea molecule in **3** could not be located. All non-hydrogen atoms were refined anisotropically except for the organic guest molecules. All hydrogen atoms were calculated at the ideal positions and refined isotropically. The crystallographic data, selected bond lengths and angles are summarized in Table 1 and Table 2.

Table 1. Crystallographic data for compounds **2** and **3**.

	2	**3**
Crystal system	monoclinic	monoclinic
Space group	$P2_1/c$	$P21/c$
Empirical formula	$C_{32}H_{21}In_3N_2O_{18}$	$C_{32}H_{19}In_3N_2O_{18}$
Formula mass	1065.97	1063.95
a [Å]	7.203(6)	7.2104(13)
b [Å]	13.43(3)	13.637(2)
c [Å]	17.54(3)	17.379(3)
β [°]	100.76(11)	100.657(7)
V [Å]^3	1666.8(4)	1679.3(5)
Z	2	2
$D_{calcd.}$ [g·cm^{-3}]	2.124	2.104
μ [mm^{-1}]	2.147	2.131
R_1 [$I > 2\sigma(I)$][a]	0.0508	0.0753
wR_2 (all data)[a]	0.1163	0.1784

[a] $R_1 = \Sigma(||F_o| - |F_c||)/\Sigma|F_o|$, and $wR_2 = \{\Sigma w[(F_o^2 - F_c^2)^2]/\Sigma w[(F_o^2)^2]\}^{1/2}$.

Table 2. Selected bond lengths and angles for compounds **2** and **3**.

Bond lengths	[Å]	Angles	[°]
Compound **2**			
In1–O2C[a]	2.094(5)	O2F–In1–O7E	90.8(2)
In1–O7	2.157(5)	O2F–In1–O9	87.5(2)
In1–O9	2.198(4)	O7–In1–O9	86.6(2)
In2–O8A	2.129(5)	O8A–In2–O4C	98.9(2)
In2–O4C	2.174(6)	O8A–In2–O9	172.3(2)
In2–O9	2.203(5)	O4C–In2–O3D	148.9(2)
In2–O3D	2.208(5)	O9–In2–O6	94.5(2)
In2–O6	2.263(5)	O9–In2–O5	90.4(2)
In2–O5	2.275(6)	O4C–In2–O9B	75.9(2)
In2–O9B	2.314(5)	O3D–In2–O6	132.7(2)
Compound **3**			
In1–O2C	2.092(6)	O2F–In1–O7E	90.9(2)
In1–O7	2.147(6)	O2F–In1–O9	87.8(2)
In1–O9	2.196(6)	O7–In1–O9	86.3(2)
In2–O8A	2.125(6)	O8A–In2–O4C	99.0(2)
In2–O4C	2.166(6)	O8A–In2–O9	173.0(2)
In2–O9	2.199(5)	O4C–In2–O3D	149.0(2)
In2–O3D	2.200(6)	O9–In2–O6	94.1(2)
In2–O6	2.264(7)	O9–In2–O5	90.7(2)
In2–O5	2.267(7)	O4C–In2–O9B	75.7(2)
In2–O9B	2.308(6)	O3D–In2–O6	132.7(2)

[a] Symmetry code: A 1 + x, y, z; B 1 – x, 1 – y, –z; C x, 1.5 – y, –0.5 + z; D 1 – x, –0.5 + y, 0.5 – z; E –x, 1 – y, –z; F –x, –0.5 + y, 0.5 – z; G –x, 0.5 + y, 0.5 – z; H x, 1.5 – y, 0.5 + z; I 1 – x, 0.5 + y, 0.5 – z.

Acknowledgement

This work was supported by grants from the National Nature Science Foundation of China (No. 20231020) and the Nature Science Foundation of Fujian Province.

[1] a) E. Y. Choi, S. Y. Kim, Y. Kim, K. Seff, *Microporous Mesoporous Mater.* **2003**, *62*, 201–210; b) X. M. Zhang, M. L. Tong, H. K. Lee, X. M. Chen, *J. Solid State Chem.* **2001**, *160*, 118–122; c) K. S. Min, M. P. Suh, *J. Am. Chem. Soc.* **2000**, *122*, 6834–6840.

[2] a) K. Biradha, Y. Hongo, M. Fujita, *Angew. Chem. Int. Ed.* **2002**, *41*, 3395–3398; b) E. Y. Lee, M. P. Suh, *Angew. Chem. Int. Ed.* **2004**, *43*, 2798–2801; c) T. J. Prior, M. J. Rosseinsky, *Inorg. Chem.* **2003**, *42*, 1564–1575; d) X. Liu, J. H. Guo, W. J. Zheng, D. Z. Liao, *Chin. J. Struct. Chem.* **2002**, *21*, 347–351.

[3] a) R. Kitaura, K. Fujimoto, S. Noro, M. Kondo, S. Kitagawa, *Angew. Chem. Int. Ed.* **2002**, *41*, 133–135; b) R. Q. Zou, X. H. Bu, R. H. Zhang, *Inorg. Chem.* **2004**, *43*, 5382–5386; c) M. P. Suh, J. W. Ko, H. J. Choi, *J. Am. Chem. Soc.* **2002**, *124*, 10976–10977; d) M. Eddaoudi, J. Kim, N. Rosi, D. Vodak, J. Wachter, M. O'Keeffe, O. M. Yaghi, *Science* **2002**, *295*, 469–472.

[4] a) O. M. Yaghi, G. Li, H. Li, *Nature* **1995**, *378*, 703–706; b) O. M. Yaghi, C. E. Davis, G. Li, H. Li, *J. Am. Chem. Soc.* **1997**, *119*, 2861–2868; c) S. S. Y. Chui, S. M. F. Lo, J. P. H. Charmant, A. G. Orpen, I. D. Williams, *Science* **1999**, *283*, 1148–1150; d) C. J. Kepert, M. J. Rosseinsky, *Chem. Commun.* **1998**, 31–32.

[5] a) H. Kumagai, C. J. Kepert, M. Kurmoo, *Inorg. Chem.* **2002**, *41*, 3410–3422; b) S. O. H. Gutschke, D. J. Price, A. K. Powell, P. T. Wood, *Eur. J. Inorg. Chem.* **2001**, 2739–2741.

[6] a) J. R. Su, K. L. Yin, D. J. Xu, *Chin. J. Struct. Chem.* **2004**, *23*, 399–402; b) J. Kim, B. L. Chen, T. M. Reineke, H. L. Li, M. Eddaoudi, D. B. Moler, M. O'Keeffe, O. M. Yaghi, *J. Am. Chem. Soc.* **2001**, *123*, 8239–8247; c) H. Kumagai, K. W. Chapman, C. J. Kepert, M. Kurmoo, *Polyhedron* **2003**, *22*, 1921–1927.

[7] a) F. D. Rochon, G. Massarweh, *Inorg. Chim. Acta* **2000**, *304*, 190–198; b) F. Jaber, F. Charbonnier, R. Faure, *J. Chem. Crystallogr.* **1997**, *27*, 397–400; c) R. Cao, Q. Shi, D. F. Sun, M. C. Hong, W. H. Bi, Y. J. Zhao, *Inorg. Chem.* **2002**, *41*, 6161–6168.

[8] a) M. Sanselme, J. M. Grenèche, M. Riou-Cavellec, G. Ferey, *Chem. Commun.* **2002**, 2172–2173; b) R. Murugavel, D. Krishnamurthy, M. Sathiyendiran, *J. Chem. Soc., Dalton Trans.* **2002**, 34–39; c) M. L. Hu, D. P. Cheng, J. G. Liu, D. J. Xu, *J. Coord. Chem.* **2001**, *53*, 7–13.

[9] a) M. Eddaoudi, J. Kim, M. O'Keeffe, O. M. Yaghi, *J. Am. Chem. Soc.* **2002**, *124*, 376–377; b) C. Serre, F. Millange, C. Thouvenot, M. Nogues, G. Marsolier, D. Louer, G. Ferey, *J. Am. Chem. Soc.* **2002**, *124*, 13519–13526.

[10] a) D. F. Sun, R. Cao, W. H. Bi, J. B. Weng, M. C. Hong, Y. C. Liang, *Inorg. Chim. Acta* **2004**, *357*, 991–1001; b) C. D. Wu, C. Z. Lu, D. M. Wu, H. H. Zhuang, J. S. Huang, *Inorg. Chem. Commun.* **2001**, *4*, 504–506; c) C. D. Wu, C. Z. Lu, W. B. Yang, S. F. Lu, H. H. Zhang, J. S. Huang, *Eur. J. Inorg. Chem.* **2002**, *4*, 797–800.

[11] Submitted for publication, crystallographic data: monoclinic, space group $P2_1/c$, a = 18.5774(19), b = 7.222, c = 21.4155(15) Å, β = 125.187(6)°, V = 125.187(6) Å^3.

[12] a) N. Audebrand, S. Raite, D. Louer, *Solid State Sci.* **2003**, *5*, 783–794; b) E. Jeanneau, N. Audebrand, D. Louer, *J. Solid State Chem.* **2003**, *173*, 387–394; c) J. Y. Sun, L. H. Weng, Y. M. Zhou, J. X. Chen, Z. X. Chen, Z. C. Liu, D. Y. Zhao, *Angew. Chem. Int. Ed.* **2002**, *41*, 4471–4473.

[13] N. E. Brese, M. O'Keeffe, *Acta Crystallogr., Sect. B.* **1991**, *47*, 192–197.

[14] L. Spek, *A Multipurpose Crystallographic Tool*, Utrecht University, Utrecht, The Netherlands, **1999**.

[15] $\{Ca_{0.5}[In_3(btec)_2(OH)_2]\cdot L\cdot 5H_2O\}_n$: $C_{26}H_{23}Ca_{0.5}In_3NO_{23}$ (1081.7) calcd. C 28.84, H 2.15, N 1.30; found C 29.65, H 2.10, N 1.21. $\{Ba_{0.5}[In_3(btec)_2(OH)_2]\cdot L\cdot 5H_2O\}_n$: $C_{26}H_{23}Ba_{0.5}In_3NO_{23}$ (1130.4) calcd. C 27.60, H 2.06, N 1.24; found C 27.42, H 1.82, N 1.30. $\{Ca_{0.5}[In_3(btec)_2(OH)_2]\cdot L'\cdot 5H_2O\}_n$: $C_{26}H_{23}Ca_{0.5}In_3NO_{23}$ (1081.7) calcd. C 28.84, H 2.35, N 1.30; found C 27.69, H 2.10, N 1.19. $\{Ba_{0.5}[In_3(btec)_2(OH)_2]\cdot L'\cdot 5H_2O\}_n$: $C_{26}H_{23}Ba_{0.5}In_3NO_{23}$ (1130.4) calcd. C 27.60, H 2.06, N 1.24; found C 25.82, H 1.80, N 1.18. L = 2-picoline, L′ = 4-picoline.

[16] The crystallographic data for compound **1** were poor, and an attempt to get high quality crystals of **1** under other conditions was unsuccessful. Thus the crystal data and crystal description of compound **1** are not available.

[17] a) G. M. Sheldrick, *SHELXS97*, *Program for Crystal Structure Solution*. University of Göttingen, Göttingen, Germany, **1997**; b) G. M. Sheldrick, *SHELXL97*, *Program for Crystal Structure Refinement*, University of Göttingen, Göttingen, Germany, **1997**.

Received: November 21, 2004

